Available online at www.sciencedirect.com

ScienceDirect

journal homepage: www.elsevier.com/locate/he

High performance of ceramic current collector fabricated at 550 °C through in-situ joining of reduced $Mn_{1.5}Co_{1.5}O_4$ for metal-supported solid oxide fuel cells

*Jiu-Tao Gao, Jia-Hong Li, Qi-Yan Feng, Chang-Jiu Li, Cheng-Xin Li**

State Key Laboratory for Mechanical Behavior of Materials, School of Materials Science and Engineering, Xi'an Jiaotong University, Xi'an, Shaanxi, China

HIGHLIGHTS

- A high-porosity current collector layer is fabricated at 550°C.
- The real working state of the current collector layer is reproduced.
- The gas distribution is simulated for designing a current collector layer.

ARTICLE INFO

Article history:
Received 11 May 2020
Received in revised form
20 June 2020
Accepted 23 June 2020
Available online xxx

Keywords:
Current collector layer
$Mn_{1.5}Co_{1.5}O_4$ (MCO)
Low temperature forming
Gas distribution

ABSTRACT

A well-connected and high-porosity current collector layer fabricated at a low temperature of 550 °C is designed for metal-supported solid oxide fuel cells (SOFCs). Reduced $Mn_{1.5}Co_{1.5}O_4$ (MCO) powders are used as the binder through the reforming of MCO in the air atmosphere. A high conductivity phase $La_{0.6}Sr_{0.4}Co_{0.2}Fe_{0.8}O_3$ (LSCF) is added to keep the porous frame microstructure and decease the ohmic polarization of the current collector layer. Three current collector layers are prepared: MCO, MCO/LSCF, and LSCF. The working state of each current collector layer in planar SOFC stack is reproduced by special experimental design; the performance is tested in the range of 550–750 °C. The results show that the current collector layer for SOFC is achieved at low temperatures using the reduction-oxidation properties of MCO, and the performance is improved by adding high conductivity phase LSCF. The gas distribution at the cathode side is also simulated for designing a high performance SOFC.

Introduction

Solid oxide fuel cells (SOFCs) are all-solid-state devices which can directly convert chemical energy stored in fuel gas to electrical energy [1–4]. Owing to the high efficiency (>65%) and low pollutant emissions, this technology is considered to be one of the most promising methods to generate sustainable energy [5,6]. As one of the development directions for SOFCs, metal-supported SOFCs (MS-SOFCs) are receiving increasing attention [5,7]. The use of metallic materials can lead to a

* *Corresponding author.*
E-mail address: licx@mail.xjtu.edu.cn (C-X. Li).

https://doi.org/10.1016/j.ijhydene.2020.06.237
0360-3199/

Please cite this article as: Gao J-T et al., High performance of ceramic current collector fabricated at 550 °C through in-situ joining of reduced $Mn_{1.5}Co_{1.5}O_4$ for metal-supported solid oxide fuel cells, International Journal of Hydrogen Energy, https://doi.org/10.1016/j.ijhydene.2020.06.237

significant reduction in the manufacturing cost of the SOFC system, which is very important for the commercialization of SOFCs [7–9]. Compared to the conventional SOFCs (i.e. anode-supported or electrolyte-supported), MS-SOFCs not only cost less but also offer other advantages, such as higher redox cycles resistance, higher electrical and thermal conductivity, and ease assembly. However, MS-SOFCs also have some limitations [9,10]: the porous metal support is easily oxidized at high temperatures. The preparation of conventional SOFC system has many processes that require a high temperature treatment; the preparation of the current collector layer is one of them.

Generally, the role of the current collector layer, especially for the cathode, is extremely important in a planar SOFC system [11–13]. Studies have shown that the quality of the cathode current collector layer greatly affects the output efficiency of the entire SOFC system [14–17]. An additional current collector layer used between the cathode and the interconnector can increase the electrode-interconnect contact area and compensate the dimensional tolerance of the parts, which makes the overall area specific resistance (ASR) decreased drastically [18–20]. The current collector technique needs to be cost-effective and efficient, as well as have good fabricability, great contact with cathode, and minimal gas diffusion resistance. Noble metals such as Ag, Au, and Pt not only have great resistance to oxidation at high temperatures, high electrical conductivity and good ductility, but also have outstandingly sinterable when they are made in fine powder form [21,22]. But the cost of these materials is too high. $La_{0.6}Sr_{0.4}Co_{0.2}Fe_{0.8}O_3$ (LSCF) and $LaNiO_3$ (LNO) [23] are the typical materials used for the cathode current collector layer of SOFCs. During the SOFC system assembly, the cathode current collector paste is applied to the cathode surface to reduce the contact resistance between the cell and the next interconnector. To increase the conductivity of the cathode current collector layer, the paste layer needs to be sintered at a very high temperature (>1000 °C) [24] which is too high for a metal porous support. Hence, how to prevent this situation is a question that needs to be addressed urgently. Yang et al. [25] reported that a $(Mn,Co)_3O_4$ spinel with a composition of $Mn_{1.5}Co_{1.5}O_4$ (MCO) can be used as a protection layer for ferritic stainless steel interconnects, owing to its excellent electrical conductivity, satisfactory thermal and structural stability, as well as good suitable expansion [26,27]. Hu et al. [28,29] reported that dense MCO coatings for interconnector protection can be prepared by atmerspheric plasma spraying (APS), and the reduction-oxidation properties of MCO at low temperatures could be utilized. These results show that MCO has the potential to be used as the current collector layer for the cathode and achieve low temperature sintering.

In this study, a new type of cathode collector layer is designed which can be formed at very low temperatures. By experimental design, the working state of the cathode current collector layer is reproduced. The performance of three different constituent layers is compared using electrochemical impedance spectroscopy (EIS) analysis. As a result, the cathode current collector layer formed at low temperatures is achieved using the reduction-oxidation properties of MCO. The reasons for the difference in the performance of different layers are elucidated. To further analyze the impact of the current collector structure on SOFC performance, the gas distribution at the cathode side is simulated.

Experiments

Experimental design

For planar SOFC stacks, a series structure is generally used for assembly. To reduce losses during current conduction, a current collector layer is applied to the surface of the cathode, as shown in Fig. 1(a); this reduces the contact resistance between the cathode and the interconnector. The current collector layer requires a certain amount of porosity to allow the gas to be transferred to the cathode while ensuring the conduction of current. The areas of the current collector layer that are in contact with the interconnector are significant, known as special areas; these areas have the highest current density and the highest resistance for gas transfer. Therefore, the performance of these areas can be used to measure the overall performance of the current collector layer. The experiment in this study is based on this design, as shown in Fig. 1.

In this experiment, the width of the special area was assumed to be 2 mm. The experiment was designed using the symmetry of the special area, as shown in Fig. 1(b). First, a symmetrical cathode with a diameter of 10 mm was prepared on the surface of an Sc_2O_3-stabilized ZrO_2 (ScSZ) electrolyte disc with a diameter of 20 mm and a thickness of 1 mm by APS (GDP-80, Jiujiang, 80 kW class). Thin sheets of aluminum oxide with a diameter of 8 mm and a thickness of 300 μm were then placed on the cathode surface. Finally, the surface of the cathode was coated with a paste of the current collector layer. Silver slices with a diameter of 10 mm were used to guide the current.

Experimental materials and characterization

MCO powders (15–55 μm) were first reduced in a hydrogen atmosphere at 800 °C for 2 h. Terpineol (Sinopharm Chemical Reagent Co., Ltd) was used as the solvent in this experiment. Silver paste as the current collector layer was used as an ideal control group. Three other pastes for the current collector layers with different compositions were configured in this experiment, as detailed in Table 1. LSCF powder with a particle size distribution of 10–50 μm was used. During the test, the samples were held in an air atmosphere at 550 °C for 5 h, and then the results were recorded by using an impedance analyzer (Solartron SI 1260/1287) under open-circuit voltage (OCV) condition. The cross-section of current collector layers was observed using field emission scanning electron microscopy (MIRA3 LMH, TESCAN, Czech Republic).

Results and discussion

Microstructure

Fig. 2 shows the microstructure of different current collector layers after testing the electrochemical properties. The cross-section of the MCO current collector layer is shown in Fig. 2(a).

Please cite this article as: Gao J-T et al., High performance of ceramic current collector fabricated at 550 °C through in-situ joining of reduced $Mn_{1.5}Co_{1.5}O_4$ for metal-supported solid oxide fuel cells, International Journal of Hydrogen Energy, https://doi.org/10.1016/j.ijhydene.2020.06.237

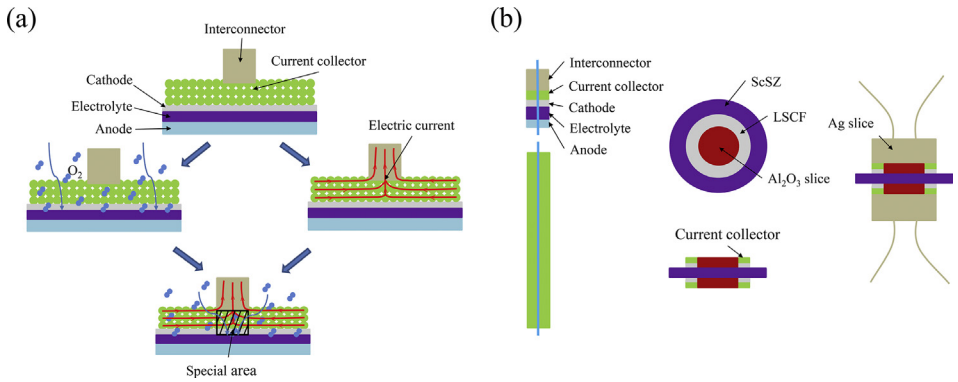

Fig. 1 – Schematic representation of the experiment: (a) function of current collector layer in planar SOFC system; (b) experiment design.

Table 1 – Detailed information of current collector pastes in the experiment.

No.	Constituents	Notes
1	Silver paste	Shanghai Synthetic Resin Research Institute
2	MCO + solvent (50 + 50) wt%	Solvent: terpineol
3	LSCF/MCO + solvent (25/25 + 50) wt%	Solvent: terpineol
4	LSCF + solvent (50 + 50) wt%	Solvent: terpineol

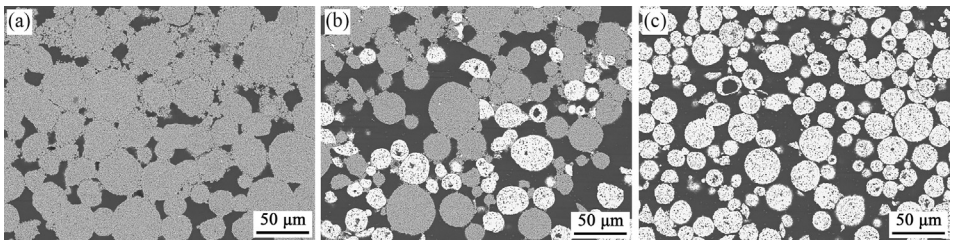

Fig. 2 – Microstructure of different current collector layers: (a) MCO; (b) LSCF/MCO; (c) LSCF.

The adjacent MCO particles have bonded together to achieve the purpose of the experimental design. It has been reported that MCO increases in mass by more than 30% with a corresponding volume expansion from the reduced state to the oxidized state [29]. Therefore, while a current collector layer containing only MCO particles may be well formed at low temperatures, but the final current collector layer structure is relatively dense, as seen in Fig. 2(a). Fig. 2(b) shows the cross-section of the current collector layer consisting of MCO and LSCF. The adjacent MCO particles are joined together, whereas the LSCF particles are held together. Owing to the presence of LSCF, this current collector layer retains a porous structure while being formed at a low temperature. The cross-section of the LSCF current collector layer is shown in Fig. 2(c). Owing to the high sintering temperature, the adjacent LSCF particles do not form effective connections at low temperatures. The current collector layer of this component can be not formed at a low temperature; it is expected that the resistance of this current collector layer will be very high. Using ImageJ software, the porosity of the different current collector layers (i.e. MCO, MCO/LSCF, LSCF) was analyzed, and the results are 0.20, 0.32, and 0.36, respectively.

Polarization

Fig. 3 shows EIS curves of different current collector layers at different temperatures. The sweeping frequency range is 0.1–10^5 Hz at an amplitude of alternating circuit (AC) voltage of 20 mV. The intercept of the high frequency impedance represents the ohmic resistance (Ro) caused by the electrolyte and the current collector layer [30]. The intercept between the high and low frequency is polarization resistance (Rp). Here, the focus is on comparing the size of the ohmic resistance and the polarization resistance of the half cells. Compared to the ideal group (silver paste), the Ro values of the half cells increase regardless of which current collector layer is used. In particular, the Ro of the half cell with the LSCF current collector layer increases dramatically. Based on the cross-section observations, the reason behind this phenomenon is that the LSCF current collector layer is not formed in the testing temperature range. In the current collector layer, the LSCF particles are independent of each other, and hence the effective conductivity of this layer is very low, resulting in a large Ro value. For a more intuitive comparison, the Ro and Rp values of the half cells with different current collector layers at

Please cite this article as: Gao J-T et al., High performance of ceramic current collector fabricated at 550 °C through in-situ joining of reduced $Mn_{1.5}Co_{1.5}O_4$ for metal-supported solid oxide fuel cells, International Journal of Hydrogen Energy, https://doi.org/10.1016/j.ijhydene.2020.06.237

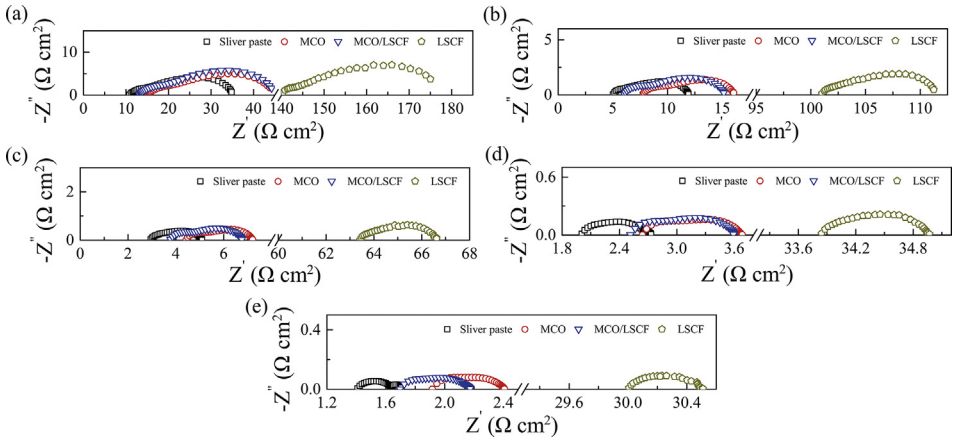

Fig. 3 – EIS results at different testing temperatures: (a) 550 °C; (b) 600 °C; (c) 650 °C; (d) 700 °C; (e) 750 °C.

different testing temperatures, obtained from Fig. 3, are shown in Fig. 4(a). As the testing temperature increases, the values of Ro and Rp decrease for each half cell. This corresponds to the fact that the conductivity and catalytic activity of materials in the system increases with temperature. It can also be seen from Fig. 4(a) that below 650 °C, the effect of Rp is larger, while above 650 °C, the effect of Ro seems to be larger. As this paper mainly studies the performance of different current collector layers after removing the electrolyte-caused resistance, Fig. 4(b) is shown to compare the change of values of Ro and Rp with different current collector layers. Here, the electrolyte thickness is assumed to be 80 μm (i.e. 1/12.5 of the ScSZ disc thickness), and the proportion of increase is calculated accordingly. It is observed that for the half-cells with different current collector layers, the proportion of Ro increase is greater than that of Rp. Owing to the massively increasing proportion of the LSCF layer Ro, this curve is not shown in Fig. 4(b). The increasing proportion of Rp is less than 80%, but the increasing proportion of Ro is more than 120%. This indicates that the conductivity of the current collector layer is of significant importance for the performance of the SOFC system.

Mechanism

Three current collector layers with paste of different compositions were tested in this experiment. Fig. 5 shows the schematic representation of the mechanism of this experiment. It has been reported that the reduction-oxidation of the $(Mn,Co)_3O_4$ spinel starts at 400 °C [29]. Hu et al. [28,29] prepared MCO interconnector protection coatings by APS and densified them through heat treatment using the MCO reduction-oxidation properties. The results of this work have shown that the current collector layer consisting of MCO can be formed at low temperatures. Fig. 5(a) shows the basic process of MCO particles for bonding at low temperatures. First, the MCO particles are treated with a reduction treatment and two phases (i.e. MnO and Co) appear on the surface. Then, these reduced particles are put together and heated in air. Finally, owing to element diffusion and phase transformation, the adjacent particles grow together. Fig. 5(b) shows the schematic representation of the MCO layer. The reduced MCO particles are easily joined together at low temperatures. However, it has been reported that the conductivity of MCO is about 100 S cm^{-1} at 800 °C [31], while the conductivity of LSCF is about 300 S cm^{-1} [32,33] at the same temperature. Therefore, it is expected that the conductivity of the pure MCO current collector layer will be lower than the conventional current collector layer (i.e. high temperature sintered LSCF), and the final dense structure will adversely affect the diffusion of oxygen to cathode. Fig. 5(c) shows the schematic representation of the MCO/LSCF layer. Based on the realization of low temperature forming, the introduction of a high conductivity phase not only improves the conductivity of the current

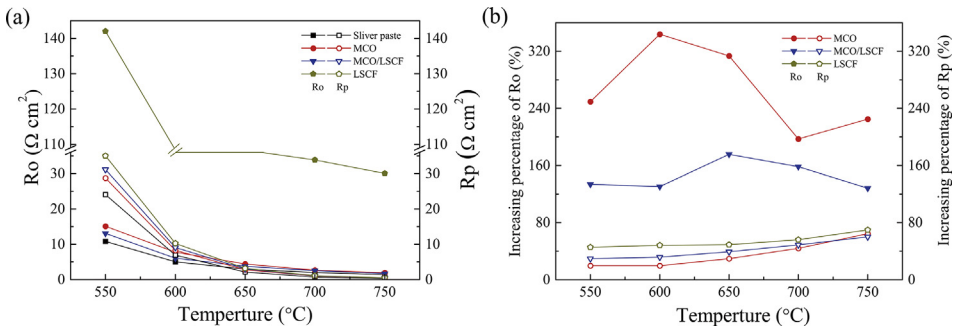

Fig. 4 – Ro and Rp of half cells with different current collector layers at different operating temperatures: (a) values; (b) change tendency.

Please cite this article as: Gao J-T et al., High performance of ceramic current collector fabricated at 550 °C through in-situ joining of reduced $Mn_{1.5}Co_{1.5}O_4$ for metal-supported solid oxide fuel cells, International Journal of Hydrogen Energy, https://doi.org/10.1016/j.ijhydene.2020.06.237

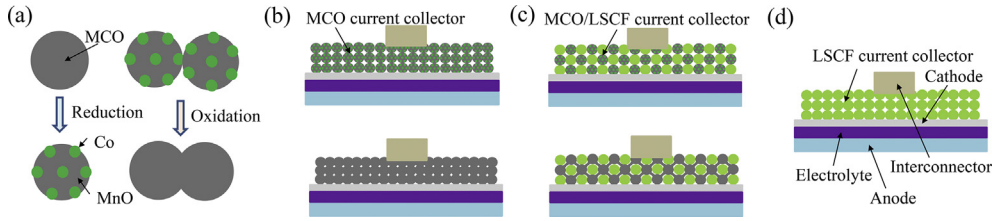

Fig. 5 – Schematic representation of the principle of this experiment: (a) MCO powder bonding process; (b) MCO current collector; (c) MCO/LSCF current collector; (d) LSCF current collector.

collector layer, but also allows the layer to retain a sufficient number of pores. Fig. 5(d) shows the schematic representation of the LSCF layer. If the current collector layer contains only LSCF particles, it cannot be formed at low temperatures owing to its high sintering temperature. The LSCF current collector layer shows a greater resistance although LSCF has a high conductivity. This is consistent with the results in Fig. 4(b).

Gas transfer and performance

According to the experimental results, different current layers seem to have little difference in the effect on the Rp of the half cells. It is possible that the large particle size of the powders used in this experiment masks this effect. In fact, the porosity of the current collector layer has a very large impact on the performance of SOFC, which directly affects the diffusion of oxygen to the cathode. Generally, mass transfer in porous media is complex and difficult to describe by the exact equations. It is commonly acknowledged that the mass transfer is based on three transmission mechanisms, which include the Knudsen diffusion, molecular diffusion and viscous flow [34–36]. Among the three mechanisms, Knudsen diffusion and molecular diffusion depend on the concentration gradient, and viscous flow is associated with the convective flow.

The diffusion mechanism mainly depends on the dimensionless quantity which is called the Knudsen number [37]. The Knudsen number is a specific value of the molecular average free path to average pore diameter [38]. If the Knudsen number is significantly greater than 10, it means that the average pore diameter is significantly larger than the molecular average free path. At this moment, the average time of collision between the molecules is much smaller than the collision on the pore wall. In this way, the Knudsen diffusion dominates the mass transfer and the influence of the molecular diffusion and viscous flow could be ignored. When the Knudsen number is below 0.1, the collision between the molecules dominates the mass transfer, which suggests that the effect of molecular diffusion and viscous flow is much higher. For the conventional current collector layer of SOFC, the pore diameter is approximately 0.2–1 μm, and the molecular average free path is approximately 0.2 μm, which implies that the Knudsen number is between 0.1 and 10. Therefore, all three kinds of mass transfer mechanisms should be considered.

It is commonly acknowledged that Fick's model (FM), Maxwell-Stefan model (MSM), and Dusty gas model (DGM) [39] are considered as the controlled function in simulation of mass transfer in SOFC. FM is simple and easy to calculate, however, it is used to describe the mass transfer in the free space and the model is only suitable for the two-component dilute solution system mass transfer and not for the SOFC mass transfer. Therefore, FM must be amended before it is used in the porous mass transfer situation [40]. MSM is an improved model which describes the mass transfer more precisely than FM. MSM is based on the theory of molecular dynamics. Assuming the collision between the molecules is inelastic, the gas diffusion could be described by the derivation of the mass conservation equation and the momentum conservation equation. MSM is a more precise model to describe mass transfer in a specific space. However, it does not consider the molecular collision on the wall. Thus, it is usually given as a governing function to describe mass transfer in a substrate where the Knudsen number is significantly lower than 0.1 (i.e. Knudsen diffusion could be ignored). Hence, it is not fully suitable for SOFC. DGM is an appropriate and precise equation to describe the mass transfer in porous electrodes. Unlike FM and MSM which do not consider the effects of porosity, DGM considers the effects of molecule-wall collisions. The principle of DGM is to treat the solid area as the $(n+1)^{th}$ component, then based on the theory of MSM, DGM could be given by the following modality [41]:

$$-\frac{dc_i}{dz} = \sum_{j=1}^{n} \frac{x_j N_i - x_i N_j}{D'_{ij}} + \frac{N_i}{D'_{iK}} \tag{1}$$

$$N_i = c_i u_i \tag{2}$$

$$N_j = c_j u_j \tag{3}$$

$$D'_{ij} = \frac{1}{\varepsilon} D_{ij} \tag{4}$$

$$D'_{iK} = \frac{D_{i(n+1)}}{1-\varepsilon} \tag{5}$$

where N_i and N_j are mole flow of component i and component j, respectively, c_i and c_j are the mole concentration of component i and component j, respectively, u_i and u_j are the absolute velocity relative to the stationary coordination, ε is the porosity of electrodes, D'_{iK} is the Knudsen diffusion coefficient, $D_{i(n+1)}$ is the binary mutual diffusion coefficient between i phase and the solid phase (i.e. (n+1) phase).

The equations above describe the influence of the difference of pressure upon mass transfer and do not take into

Please cite this article as: Gao J-T et al., High performance of ceramic current collector fabricated at 550 °C through in-situ joining of reduced $Mn_{1.5}Co_{1.5}O_4$ for metal-supported solid oxide fuel cells, International Journal of Hydrogen Energy, https://doi.org/10.1016/j.ijhydene.2020.06.237

consideration the function of viscous flow. Thus, when considering the influence of viscous flow, the equations must be amended to add the viscous convection item:

$$N_i' = N_i + N_v = N_i + x_i \frac{p}{RT}\left(-\nabla p \frac{k}{\mu}\right) \tag{6}$$

where N_v is the viscous flow item, p is the pressure in the porous electrode, k is the permeability, μ is the dynamic viscosity. After the improvement of the equations, DGM could be given by:

$$\frac{N_i'}{D_{iK}^{eff}} + \sum_{j=1}^{n} \frac{x_j N_i' - x_i N_j'}{D_{ij}^{eff}} = -\frac{1}{RT}\left[x_i \nabla p \frac{kp}{D_{iK}^{eff}\mu} + p\nabla x_i + x_i \nabla p\right] \tag{7}$$

where D_{ij}^{eff} and D_{iK}^{eff} are the effective binary diffusion coefficient and the effective Knudsen diffusion coefficient respectively, they could be calculated from the intrinsic diffusion coefficient, which considers the structure parameter of dynamic viscosity μ and porosity ε. In this way, the effective binary diffusion coefficient D_{ij}^{eff} could be given by Ref. [41]:

$$D_{ij}^{eff} = \frac{\varepsilon}{\tau}\frac{3.24\times10^{-8}T^{1.75}}{p\left(V_i^{1/3}+V_j^{1/3}\right)^2}\left(\frac{1}{M_i}+\frac{1}{M_j}\right)^{0.5} \tag{8}$$

where ε is porosity of electrodes, τ is tortuosity, M_i and M_j are the molar mass of component i and component j respectively, V_i is the diffusion volume for component i (V_i = 6.12 × 10^{-6} m^3 mol^{-1}, 13.1 × 10^{-6} m^3 mol^{-1}, 16.3 × 10^{-6} m^3 mol^{-1} and 18.5 × 10^{-6} m^3 mol^{-1} for H_2, H_2O, O_2, and N_2, respectively.

The effective Knudsen diffusion coefficient D_{iK}^{eff} could be given by Ref. [42]:

$$D_{iK}^{eff} = \frac{\varepsilon}{\tau}\frac{2r_g}{3}\sqrt{\frac{8RT}{\pi M_i}} \tag{9}$$

where r_g is the mean hydraulic pore radius. The Knudsen effective diffusion coefficient is significantly important when the Knudsen number is higher than 0.1, which takes into account the collision between the molecules and the wall.

Based on the theory of Darcy's law [43,44] and the process of calculability on MSM, DGM could be utilized to describe mass transfer in the porous species more precisely and accurately, and therefore, DGM becomes the most important model to calculate the gas transport and distribution in the porous electrode. In this study, COMSOL Multiphysics was used to simulate the gas distribution. The effective area of the cathode in this model is 90 × 90 cm^2. The thickness of the current collector layer is 0.3 mm and the porosity is 0.2. The widths of both the gas channel and the rib are 2 mm and the depth of gas channel is 0.5 mm. The flow rates of air and hydrogen are 1.5 slm and 0.3 slm, respectively. The working voltage is 0.7 V and the working temperature is 750 °C. The result of the gas concentration distribution field at the cathode side is shown in Fig. 6. As mentioned in section Experimental design, the area in contact with interconnector has the lowest gas concentration, which is as low as half of the gas concentration in the gas channel. In other words, there is a large gas concentration gradient inside the current collector layer. This indicates that the porosity of the current collector layer may have a big impact on the gas distribution at the cathode side. Fig. 7 shows the I–V simulation results of SOFC with different porosity current collector layers (0.1, 0.2, 0.3, and 0.4). The results of the simulation show that the cell performance decreases when the porosity of the current collector layer decreases. When the cell is operating at a high current density level, this effect will be more significant. This means that oxygen could not be adequately fed in time when the current density of the SOFC is high, as is with a low porosity current collector layer. Therefore, the porosity is important for the current collector layer especially when the SOFC is working at a high current density level. Simulation results also show that the effect on the SOFC performance in terms of gas diffusion seems to be smaller after the porosity of the current collector layer is greater than 0.2. Thus, this illustrates the importance of improving the conductivity of current collector layer.

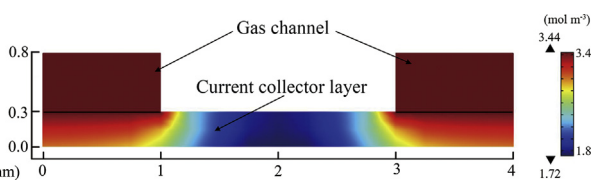

Fig. 6 – Gas concentration distribution field at cathode side.

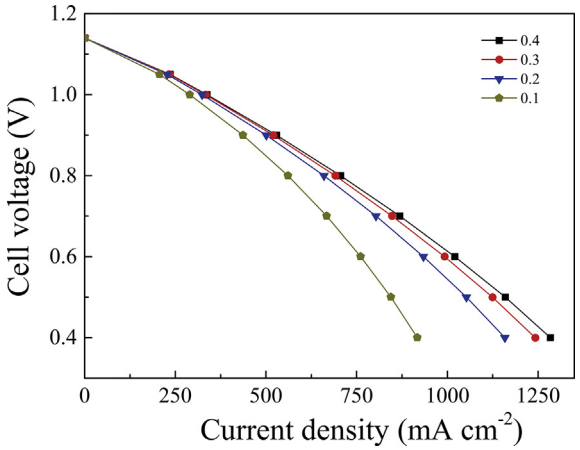

Fig. 7 – I–V simulation results of SOFC with different porosity current collector layers.

Conclusion

By exploiting the reduction-oxidation properties of MCO, this study achieves the aim of forming the SOFC current collector layer at a low temperature (550 °C). The real working state of the current collector layer in the planar SOFC stack is realized through the special experimental design. The results show that the original experimental scenario is suitable. Through the EIS testing in the range of 550–750 °C, the MCO/LSCF layer shows a better performance than the other current collector layers (i.e. MCO and LSCF). The appropriate proportion of the high conductivity phase (LSCF) in MCO helps to improve the performance of the current collector layer without affecting

Please cite this article as: Gao J-T et al., High performance of ceramic current collector fabricated at 550 °C through in-situ joining of reduced $Mn_{1.5}Co_{1.5}O_4$ for metal-supported solid oxide fuel cells, International Journal of Hydrogen Energy, https://doi.org/10.1016/j.ijhydene.2020.06.237

the low temperature formation. However, regardless of the current collector layer used, the impedance in the half cell system is increased. The results of the simulation show that the gas concentration in the current collector layer under the interconnector is as low as half of the gas concentration in the gas channel. The output performance of the SOFC decreases with the decreasing porosity of current collector layer. Therefore, the porosity of the current collector layer is also a key factor which affects the output performance of the SOFC.

Declaration of competing interest

The authors declare that they have no known competing financial interests or personal relationships that could have appeared to influence the work reported in this paper.

Acknowledgements

This work was supported by the National Key Research and Development Program of China (Basic Research Project, Grant No. 2017YFB0306100), the National Natural Science Foundation of China (Grant NO. 91860114), and the National Key Research and Development Program of China (China-USA Intergovernmental Cooperation Project, Grant NO. 2017YFE0105900).

REFERENCES

[1] Tompsett GA, Finnerty C, Kendall K, Alston T, Sammes NM. Novel applications for micro-SOFCs. J Power Sources 2000;86:376–82.
[2] Chen Y, Wang F, Chen D, Dong F, Park HJ, Kwak C, et al. Role of silver current collector on the operational stability of selected cobalt-containing oxide electrodes for oxygen reduction reaction. J Power Sources 2012;210:146–53.
[3] da Silva FS, de Souza TM. Novel materials for solid oxide fuel cell technologies: a literature review. Int J Hydrogen Energy 2017;42:26020–36.
[4] Li J, Jia L, Chi B, Pu J, Li J, Wang S. Novel gradient porous cathode for intermediate temperature solid oxide fuel cell. Int J Hydrogen Energy 2019;44:31525–30.
[5] Zhou Y, Xin X, Li J, Ye X, Xia C, Wang S, et al. Performance and degradation of metal-supported solid oxide fuel cells with impregnated electrodes. Int J Hydrogen Energy 2014;39:2279–85.
[6] Shimura T, Jiao Z, Shikazono N. Dependence of solid oxide fuel cell electrode microstructure parameters on focused ion beam – scanning electron microscopy resolution. Int J Hydrogen Energy 2016;41:22373–80.
[7] Krishnan VV. Recent developments in metal-supported solid oxide fuel cells. WIREs Energy and Environment 2017;6:e246.
[8] Fondard J, Bertrand P, Billard A, Fourcade S, Batocchi P, Mauvy F, et al. Manufacturing and testing of a metal supported Ni-YSZ/YSZ/La2NiO4 IT-SOFC synthesized by physical surface deposition processes. Solid State Ionics 2017;310:10–23.
[9] Tucker MC. Development of high power density metal-supported solid oxide fuel cells. Energy Technol 2017;5:2175–81.
[10] Dogdibegovic E, Wang R, Lau GY, Tucker MC. High performance metal-supported solid oxide fuel cells with infiltrated electrodes. J Power Sources 2019;410–411:91–8.
[11] Yang Z, Xia G, Singh P, Stevenson JW. Electrical contacts between cathodes and metallic interconnects in solid oxide fuel cells. J Power Sources 2006;155:246–52.
[12] Zhong H, Matsumoto H, Ishihara T, Toriyama A. Ag current collector for honeycomb solid oxide fuel cells using LaGaO3-based oxide electrolyte. J Power Sources 2009;186:238–43.
[13] Wang G, Guan W, Miao F, Wang WG. Factors of cathode current-collecting layer affecting cell performance inside solid oxide fuel cell stacks. Int J Hydrogen Energy 2014;39:17836–44.
[14] Hsiao YC, Selman JR. The degradation of SOFC electrodes. Solid State Ionics 1997;98:33–8.
[15] Jiang SP. Resistance measurement in solid oxide fuel cells. J Electrochem Soc 2001;148:A887.
[16] Yoon KJ, Zink P, Gopalan S, Pal UB. Polarization measurements on single-step co-fired solid oxide fuel cells (SOFCs). J Power Sources 2007;172:39–49.
[17] Kong W, Su SC, Gao X, Zhang DH, Yu ZD. Optimization of the anode current collector layer thickness for the cathode-supported solid oxide fuel cell. Adv Mater Res 2013;712–715:1325–9.
[18] Wu W, Wang GL, Guan WB, Zhen YF, Wang WG. Effect of contact method between interconnects and electrodes on area specific resistance in planar solid oxide fuel cells. Fuel Cell 2013;13:743–50.
[19] Li Q, Zheng Y, Guan W, Jin L, Xu C, Wang WG. Achieving high-efficiency hydrogen production using planar solid-oxide electrolysis stacks. International Journal of Hydrogen Energy. Int J Hydrogen Energy 2014;39:10833–42.
[20] Yang Z, Xia G, Singh P, Stevenson JW. Electrical contacts between cathodes and metallic interconnects in solid oxide fuel cells. J Power Sources 2006;155:246–52.
[21] Bai JG, Creehan KD, Kuhn HA. Inkjet printable nanosilver suspensions for enhanced sintering quality in rapid manufacturing. Nanotechnology 2007;18:185701.
[22] Moon KS, Hai D, Maric R, Pothukuchi S, Hunt A, Yi L, et al. Thermal behavior of silver nanoparticles for low-temperature interconnect applications. J Electron Mater 2005;34:168–75.
[23] Schuler JA, Wuillemin Z, Hessler-Wyser A, Comminges C, Steiner NY, Van herle J. Cr-poisoning in (La,Sr)(Co,Fe)O_3 cathodes after 10,000h SOFC stack testing. J Power Sources 2012;211:177–83.
[24] Sasaki K. Microstructure-property relations of solid oxide fuel cell cathodes and current collectors. J Electrochem Soc 1996;143:530.
[25] Yang Z, Xia G, Li X, Stevenson J. (Mn,Co)3O_4 spinel coatings on ferritic stainless steels for SOFC interconnect applications. Int J Hydrogen Energy 2007;32:3648–54.
[26] Yang Z, Xia G, Simner SP, Stevenson JW. Thermal growth and performance of manganese cobaltite spinel protection layers on ferritic stainless steel SOFC interconnects. 2005.
[27] Yang Z, Xia G, Stevenson JW. Mn[sub 1.5]Co[sub 1.5]O[sub 4] spinel protection layers on ferritic stainless steels for SOFC interconnect applications. Electrochem Solid State Lett 2005;8:A168.
[28] Hu Y-Z, Li C-X, Yang G-J, Li C-J. Evolution of microstructure during annealing of Mn1.5Co1.5O4 spinel coatings deposited by atmospheric plasma spray. Int J Hydrogen Energy 2014;39:13844–51.
[29] Hu Y-Z, Yun L-L, Wei T, Li C-X, Qi Z, Yang G-J, et al. Aerosol sprayed Mn1.5$Co_{1.5}O_4$ protective coatings for metallic interconnect of solid oxide fuel cells. Int J Hydrogen Energy 2016;41:20305–13.

Please cite this article as: Gao J-T et al., High performance of ceramic current collector fabricated at 550 °C through in-situ joining of reduced $Mn_{1.5}Co_{1.5}O_4$ for metal-supported solid oxide fuel cells, International Journal of Hydrogen Energy, https://doi.org/10.1016/j.ijhydene.2020.06.237

[30] Bian L, Duan C, Wang L, Zhu L, O'Hayre R, Chou K-C. Electrochemical performance and stability of $La_{0.5}Sr_{0.5}Fe_{0.9}Nb_{0.1}O_{3-\delta}$ symmetric electrode for solid oxide fuel cells. J Power Sources 2018;399:398–405.
[31] Yang Z, Xia G-G, Li X-H, Stevenson JW. $(Mn,Co)3O_4$ spinel coatings on ferritic stainless steels for SOFC interconnect applications. Int J Hydrogen Energy 2007;32:3648–54.
[32] Dusastre V, Kilner JA. Optimisation of composite cathodes for intermediate temperature SOFC applications. Solid State Ionics 1999;126:163–74.
[33] Xin X, Liu L, Liu Y, Zhu Q. Novel perovskite-spinel composite conductive ceramics for SOFC cathode contact layer. Int J Hydrogen Energy 2018;43:23036–40.
[34] Levitz P. Knudsen diffusion and excitation transfer in random porous media. J Phys Chem 1993;97:3813–8.
[35] Briner BG, Doering M, Rust H-P, Bradshaw AM. Microscopic molecular diffusion enhanced by adsorbate interactions. Science 1997;278:257–60.
[36] Yu D, Mei R, Luo L-S, Shyy W. Viscous flow computations with the method of lattice Boltzmann equation. Prog Aero Sci 2003;39:329–67.
[37] Wu L. A slip model for rarefied gas flows at arbitrary Knudsen number. Appl Phys Lett 2008;93:253103.
[38] Varoutis S, Naris S, Hauer V, Day C, Valougeorgis D. Computational and experimental study of gas flows through long channels of various cross sections in the whole range of the Knudsen number. J Vac Sci Technol 2008;27:89–100.
[39] Hernández-Pacheco E, Singh D, Hutton PN, Patel N, Mann MD. A macro-level model for determining the performance characteristics of solid oxide fuel cells. J Power Sources 2004;138:174–86.
[40] Suwanwarangkul R, Croiset E, Fowler MW, Douglas PL, Entchev E, Douglas MA. Performance comparison of Fick's, dusty-gas and Stefan–Maxwell models to predict the concentration overpotential of a SOFC anode. J Power Sources 2003;122:9–18.
[41] Todd B, Young JB. Thermodynamic and transport properties of gases for use in solid oxide fuel cell modelling. J Power Sources 2002;110:186–200.
[42] Veldsink JW, van Damme RMJ, Versteeg GF, van Swaaij WPM. The use of the dusty-gas model for the description of mass transport with chemical reaction in porous media. Chem Eng J Biochem Eng J 1995;57:115–25.
[43] Bove R, Ubertini S. Modeling solid oxide fuel cell operation: approaches, techniques and results. J Power Sources 2006;159:543–59.
[44] Liu S, Song C, Lin Z. The effects of the interconnect rib contact resistance on the performance of planar solid oxide fuel cell stack and the rib design optimization. J Power Sources 2008;183:214–25.

Please cite this article as: Gao J-T et al., High performance of ceramic current collector fabricated at 550 °C through in-situ joining of reduced $Mn_{1.5}Co_{1.5}O_4$ for metal-supported solid oxide fuel cells, International Journal of Hydrogen Energy, https://doi.org/10.1016/j.ijhydene.2020.06.237